Letter

Self-assembly of two-dimensional, amorphous materials on a liquid substrate

Deborah Schwarcz [*] and Stanislav Burov [†]
Physics Department, Bar-Ilan University, Ramat Gan 5290002, Israel

(Received 9 December 2021; accepted 26 January 2022; published 23 February 2022)

Recent experimental utilization of liquid substrate in the production of two-dimensional crystals, such as graphene, together with a general interest in amorphous materials, raises the following question: is it beneficial to use a liquid substrate to optimize amorphous material production? Inspired by epitaxial growth, we use a two-dimensional coarse-grained model of interacting particles to show that introducing a motion for the substrate atoms improves the self-assembly process of particles that move on top of the substrate. We find that a specific amount of substrate liquidity (for a given sample temperature) is needed to achieve optimal self-assembly. Our results illustrate the opportunities that the combination of different degrees of freedom provides to the self-assembly processes.

DOI: 10.1103/PhysRevE.105.L022601

I. INTRODUCTION

The rise of two-dimensional (2D) materials opens a variety of possibilities for materials science and nanotechnology [1–6]. It is possible to distinguish between two different categories of 2D materials: crystal and amorphous materials. While crystals have a periodic structure, amorphous materials are categorized by the lack of periodicity. Material microscopic structure has a crucial impact on its global properties; therefore, controlling the self-organization of two-dimensional materials, such as ordered or disordered graphene, is vital to optimizing their performance [7,8].

Two-dimensional materials are frequently produced by bottom-up techniques like chemical vapor deposition (CVD), plasma-enhanced CVD, or physical vapor deposition [1,9–11]. In these methods, atoms are deposited on a substrate, move on the substrate, interact, and self-assemble. The main challenge of creating 2D amorphous matter by bottom-up techniques is to obtain a large and defect-free cluster. Controlling growth parameters such as temperature, pressure, and substrate geometry enables one to fit the outcome with high reproducibility [12–18]. Recently, a liquid substrate was experimentally utilized for crystal growth. The lack of a crystallographic substrate has been observed to positively impact crystallization, i.e., larger crystal size [19–22]. It is also possible to promote the rearrangement of atoms by utilizing methods like radiation [23–27], electric/magnetic fields [28], and heating [29]. The superposition of several of the mentioned methods and their effect on interatomic interaction also has been explored. For example, thermal activation and UV radiation promote the rearrangement of atoms in glassy systems [25]. Reviews of diverse experimental methods and simulation techniques for self-assembly of nanoparticles into large clusters can be found in [28,30].

Self-assembly is a generic name for a microscopic process that determines the spontaneous self-organization of the building blocks of the material. It can be naturally stimulated or modified by controlling experimental conditions [28,31]. Previously self-assembly was explored by croase grained models such as terrace ledge kink models [32,33], the Kardar-Parisi-Zhang (KPZ) equation [34], tile assembly models [35,36], and solid on solid (SOS) models [16,37,38].

On the level of a single particle, self-assembly occurs due to interparticle interactions. In general, particles present in the vicinity of local energy minima are separated by significant energy barriers. From time to time, particles experience abrupt transitions between these local minima. These transitions occur due to random fluctuations that enable the system to escape from a metastable state [39]. We generally address random fluctuations as noise. It is possible to distinguish between two kinds of noise effects on the single particles: a uniform effect that, on average, affects all the particles similarly and a heterogeneous impact that will affect each particle differently. In this study, we develop a coarse-grained model of interacting particles (a generalization of the SOS model [16,37,38]) to explore the impact of different noises on the self-assembly processes of amorphous materials. Due to the focus on amorphous structures, by self-assembly we refer to emergence of a coarse-grained, dense aggregation of particles, and not a formation of crystalline phase. We separately introduce two kinds of noises in the model. One type has the same impact on each atom in the system; we call it uniform noise. The other noise has a different effect on each atom in the system, and hence the name local noise. The temperature is assumed to be constant across the sample; therefore, it is a uniform noise. In contrast, atoms of the liquid substrate move differently through the sample; thus, their motion causes a different substrate arrangement at each point, i.e., a local noise. The emerging questions are, What is the impact of the various noises on self-assembly processes? Which noise is beneficial for 2D self-assembly? What happens when a cohort of these noises is applied? This study explores these questions

[*] deborah.schwarcz@gmail.com
[†] stasbur@gmail.com

by simulating a self-assembly process of an amorphous cluster on top of a liquid substrate. We use molecular dynamics (MD) to describe the motion of substrate atoms and the kinematic Monte Carlo (KMC) approach to address the self-assembly of particles on top of the substrate. Voronoi tessellation representation of the substrate interlinks these two approaches.

II. MODELS AND METHODS

We simulate two-dimensional, amorphous cluster growth on top of a liquid substrate. Our model consists of a substrate and particles that move and self-assemble on top of the substrate. The substrate is a set of atoms that can reorganize. Initially, the substrate atoms are randomly dispersed. To obtain more or less uniform substrate density, we divide the sample into equal squares and randomly introduce an atom into each square. The substrate atom number i interacts with substrate atom number j via Lennard-Jones potential $V_{i,j}$:

$$V_{i,j} = 4\epsilon[(\sigma/r_{i,j})^{12} - (\sigma/r_{i,j})^{6}], \tag{1}$$

where $\epsilon = 100$, $\sigma = 10^4$, and $r_{i,j}$ is the distance between atoms i and j. The surface is a square of size $20\sigma \times 20\sigma$; periodic boundary conditions are implied. To consider only the short-ranged repulsion interaction between atoms, we cut off the potentials at 1.1σ, i.e., Weeks-Chandler-Anderson (WCA) potential (see [40]). The overdamped Langevin equation determines the dynamics of the substrate atoms, i.e., the position of the $i$ith particle is

$$\vec{r}_i(t+\Delta t) = \vec{r}_i(t) + \sqrt{D\delta t}(\eta_x\hat{x} + \eta_y\hat{y}) + \sum_{i=1}^{n} 4\epsilon\left[-12\frac{\sigma^{12}}{r_{i,j}^{13}} + 6\frac{\sigma^6}{r_{i,j}^7}\right]\delta t\,\hat{p}_{i,j}, \tag{2}$$

where $D = 1.5\times10^{-7}\sigma^2/\delta t$ is the diffusion coefficient, n is the number of particles that are closer than 1.1σ, $\delta t = 0.005$ is the time step size and $\hat{p}_{i,j}$ is the unit vector in the direction $\vec{r}_j - \vec{r}_i$. η_x and η_y simulate Gaussian noise for each axis (see the Supplemental Material [41]).

We use Voronoi tesselation [42] to define the substrate sites created by the substrate atoms. Voronoi tessellation is defined by a set of nonordered sites, i.e., a set of randomly placed points. Each site defines a cell, a Voronoi cell, that covers all the points that are closer to a given site than to any other site [42]. For a given Voronoi cell, neighbor Voronoi cells are defined as cells that share a common boundary. The number of neighbor Voronoi cells and circumference length varies between different cells; see Fig. S1 in the Supplemental Material [41]. In our model, each substrate atom represents the central point of a given Voronoi cell. Thus, the motion of substrate atoms alters the Voronoi tessellation. These modifications influence the geometry of all the cells simultaneously, but each Voronoi cell is affected uniquely. Ultimately, these unique and random rearrangements introduce local noise to the system. During our simulation, we update the Voronoi tessellation. The number of MD steps between sequential Voronoi tessellation updates should be large enough for the change in the structure to be significant. That is, nonzero modifications for the cell circumference should be observed. But at the same time, many MD steps completely modify the Voronoi tessellation and disconnect previously neighboring cells. To balance these criteria, we use a temporal step of $1800\delta t$ between sequential updates of the Voronoi tessellation. Due to interaction via the Lennard-Jones potential [Eq. (1)], the substrate atoms move significant distances during the tessellation update step. Since the substrate atoms are in equilibrium, the chosen update step of the Voronoi tessellation reflects proper sampling of the various positions of the substrate atoms. Additional possible updates of the Voronoi tessellation are discussed in the Supplemental Material [41].

The substrate structure, i.e., Voronoi tessellation, defines the possible locations and dynamics of self-assembling particles that move on top of the substrate. Each Voronoi cell can be occupied by up to one self-assembling particle. Initially, all the particles are randomly dispersed among the Voronoi cells. We use the KMC model to determine the transitions between different substrate sites of the self-assembling particles. At each iteration of the KMC, one particle can hop from one Voronoi cell to one of the unoccupied neighboring Voronoi cells. The local geometry of a given Voronoi cell determines the interaction energy of two nearby particles, i.e., self-assembling particles located at neighbor Voronoi cells. This bonding interaction depends on the length of the mutual edge of the Voronoi cell; thus the total energy of a particle situated in Voronoi cell s is provided by $E_s = -J\frac{b_s\sum_k b_k f_{s,k}}{\sum_k f_{s,k}}$, the summation is over all the neighbors of cell s, and $f_{s,k}$ is the length of the boundary between cells s and k. b_k is 1 if cell k is occupied and 0 otherwise. This definition assumes that particle-particle interactions are linear with the distance between particles since the average distance between two randomly allocated particles in two adjacent Voronoi cells is proportional to the length of their mutual boundary [18].

The probability of a particle to leave its current site and jump to one of the adjacent empty cells follows

$$p_s = e^{\beta E_s}, \tag{3}$$

where $\beta = \frac{1}{k_B T}$, T is the temperature and k_B is the Boltzmann constant. If the attempt of the particle to leave its current cell s is successful, it will consider all the potential destinations (i.e., empty neighboring cells). For each of those potential destinations the transition probability $p_{s\to k}$ is

$$p_{s\to k} = \frac{e^{-\beta\Delta E_{s,k}}}{\sum_k e^{-\beta\Delta E_{s,k}}}, \tag{4}$$

where $\Delta E_{s,k} = E_k - E_s$ and the summation is over all the potential cells k. During the simulation, self-assembling particles' locations are updated sequentially one after the other. Since the self-assembling particles are indistinguishable, it is possible to use sequential updating instead of random updating generally used in MC simulations [43]. Each N KMC steps, the Voronoi tesselation is updated according to the algorithm described above. In the following, we use the term vibration frequency $= 1/N$ to describe the periodic updates of the Voronoi tessellation. These Voronoi tesselation updates are terminated after a specific (and vast) number of KMC steps. We allow the system to relax on top of a specific (but randomly chosen) Voronoi tessellation. Notice that when such relaxation is introduced, we assume that we can control the motion of the substrate atoms. Such control is mathematically achieved via setting $D \to 0$ or rapid freezing

of the substrate. Suppose the origin of the noise that affects substrate atoms rearrangements is achieved via an external source, such as rattling of the system. In that case, the relaxation phase occurs when this external source is switched off. It is worth noting that recently a model describing ion transport processes used similar ideas of dividing the system into two coupled subsystems. MD represents one subsystem and the other is represented by MC; see [44].

The main parameter that describes "successful" self-assembly is cluster compactness. To measure the cluster compactness, we sum over the lengths of the edges of all the cells. The measure is defined by $U = \frac{1}{2}\sum_s \sum_k f_{s,k}|(b_s - b_k)|$ where b_s is 1 if cell s is occupied and 0 otherwise, s indicates different particles, and k indicates the various neighbours of particle s. Due to the presence of $|b_s - b_k|$, in U, only situations where just one of the cells (s, k) is occupied contribute to U. Since the number of particles is fixed, small U describes situations when many particles are clumped together and form clusters. Large U may be caused by holes in the cluster or the emergence of many small clusters instead of a large one. Such situations are not desirable.

III. RESULTS

Two types of noises are present in the model. The first noise is the thermal one that we term uniform. It is varied by controlling the temperature in Eqs. (3) and (4). The second noise is introduced via rearrangements of the substrate atoms. The Voronoi cells differ extensively from one place to another. Therefore the term "local noise" describes substrate variations. We vary the vibration frequency of the substrate. In Figs. 1(a)–1(c) the U with pronounced oscillations describes the situation when substrate rearrangements are introduced. The whole behavior looks as if the system is periodically rattled. As mentioned above, we stop these substrate variations after a specific amount of time (i.e., KMC steps). After the substrate vibrations are terminated, U starts to decay (on average). Surprisingly, this decay leads to terminal values of U that are smaller than the values achieved without substrate deformations, given that the measurement time is the same for both cases. This effect occurs even though at the start of the final relaxation, U for the case with local noise is larger (i.e., less compact cluster) than U for the case without such noise. In Figs. 1(a)–1(c) we present three representative cases of how U behaves for different duration of vibrations. Panel (d) summarizes the findings for different values of duration of vibrations. This improvement disappears when the vibration duration is close enough to the measurement time and the period of the relaxation phase is too short. Through this work we use $\sim\frac{1}{3}$ of the measurement time for the duration of vibrations. We notice that similar effect of positive impact due to inclusion of additional noise can be achieved when the Voronoi tessellation dynamics is modified (see the Supplemental Material [41])

The two noises affect quite differently the immediate evolution of the system. While particles temperature increase leads to consistent small fluctuations, each substrate vibration violently destabilizes the system due to the reconfiguration of intersubstrate energetic bonds. When we eliminate substrate variations and consider only the effect of temperature, i.e., uniform noise, two distinct regimes appear. For low temperatures, the system is stuck in a metastable state [Fig. 2(c)] where large "holes" persist for extremely long times in the cluster. On the other hand, for high temperatures, the system

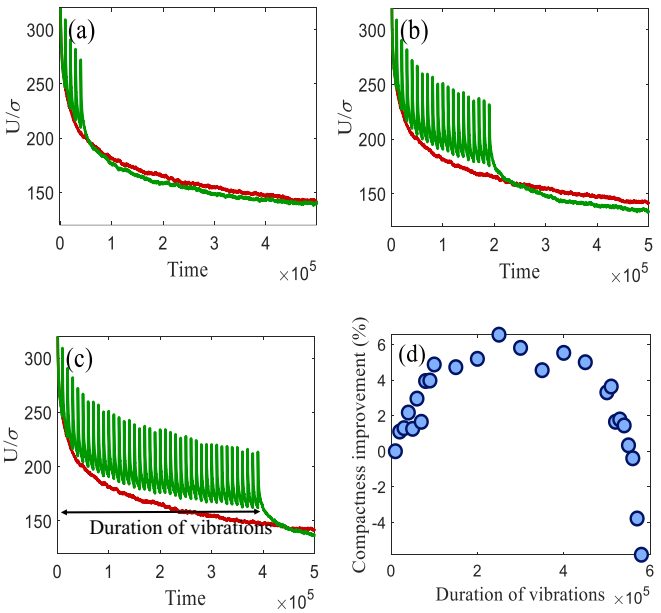

FIG. 1. (a)–(c) Compactness as a function of time for $k_BT/J = 1/7$, vibration frequency 10^{-4} and different periods of vibrations [illustrated in panel (c)]. Red curves describe the cases without substrate variations and green curves the cases where dynamical substrate variations were implemented. Durations of vibration are (a) 5×10^4 KMC steps, (b) 2×10^5 KMC steps, (c) 4×10^5 KMC steps. (d) Cluster compactness at the end of the measurement for various durations of vibration. The simulations were performed for 260 particles and 100 realizations and the measurement time was 6×10^5.

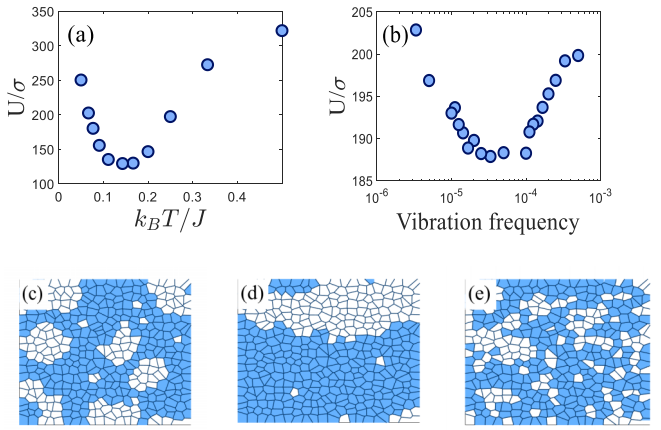

FIG. 2. (a)–(b) Cluster compactness as a function of the amount of "noise" in the system, averaging over 99 realizations. (a) Only thermal fluctuations are present. (b) Thermal fluctuations and substrate variations are present and the temperature is fixed, $k_BT/J = 1/15$. (c)–(e) Snapshots of the formed cluster with no substrate variations; the straight lines determine the boundary of every Voronoi cell. (c) $k_BT/J = 1/15$. (d) $k_BT/J = 1/7$. (e) $k_BT/J = 1/3$. 260 particles were used and the measurement time was 6×10^6 KMC steps.

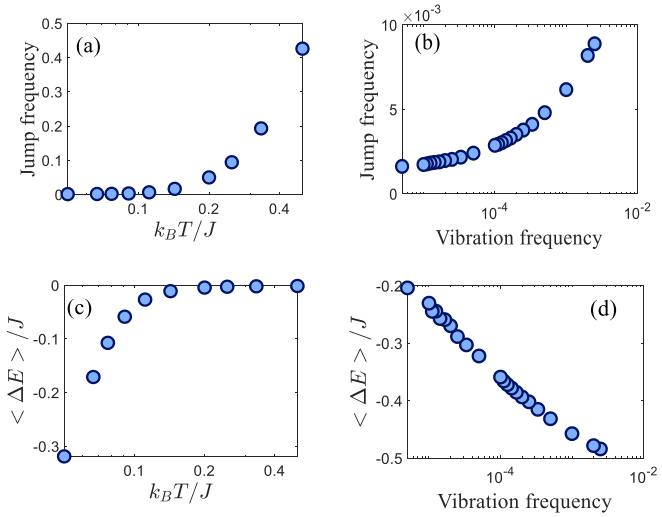

FIG. 3. Single-particles behavior during cluster formation. (a) Jump frequency as a function of temperature and no substrate vibrations. (b) Jump frequency as a function of vibration frequency and fixed temperature $k_BT/J = 1/15$. (c) Energetic gain as a function of temperature and no substrate vibrations. (d) Energetic gain as a function of vibration frequency and fixed temperature $k_BT/J = 1/15$. The measurement time was 10^6 KMC steps, with 260 particles and averaging over 100 realizations.

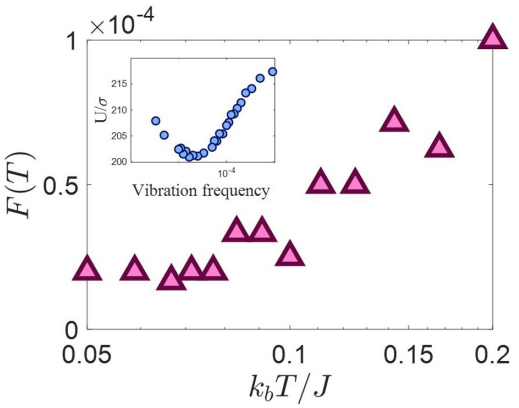

FIG. 4. Optimal vibration frequency $F(T)$ as a function of temperature. For each temperature the minimum of U as a function of vibration frequency was detected (see the inset). The measurement time was 6×10^6 KMC steps, with 300 particles and averaging over 1000 realizations.

stays in a homogeneous phase. Local formation of cluster grains are disassembled very fast [Fig. 2(e)]. In both high- and low-temperature limits, U is large. There is an optimal intermediate temperature where some balance is reached between the tendency to break loose and the opportunity to stay locally connected. For this optimal temperature U reaches a minimal value, as shown in Fig. 2(a), and a compact cluster is obtained [Fig. 2(d)]. This result agrees with previous findings where an optimal interaction that leads to an efficient self-assembly process was observed [45,46].

When the temperature is set to be constant, and the vibration frequency is modified, a similar effect is observed. Figure 2(b) shows that U behaves nonmonotonically with vibration frequency. The small vibration frequency of the substrates acts beneficially, up to a specific limit. Further inclusion of additional noise is destructive for cluster formation. Comparison of panels (a) and (b) in Fig. 2 shows that the roles of vibration frequency and temperature are close. The dynamic range of the y axis in Figs. 2(a) and 2(b) discloses that the size of the impact of the noises is different: temperature has much more effect on cluster compactness than substrate variations.

To better characterize the differences and the similarities of the impact of the two noises, we explore the single-particle behavior. We define jump frequency as the total number of transitions between different Voronoi cells performed by the self-assembling particles, divided by the measurement, i.e., total number of KMC steps. Panel (a) of Fig. 3 shows that the jump frequency monotonically grows with the temperature when there are no substrate variations. Similar behavior of the jump frequency appears when the temperature is kept fixed, and the vibration frequency is modified, Fig. 3(b). Again, the scales of the panels disclose that the effect of temperature modifications is superior to variations of the vibration frequency. This increase in jump frequency due to the rise of the noise, either uniform or local, is expected. The jump frequency is associated with a kinetic energy that grows when the temperature is increased. Moreover, the increase of temperature generally allows a system to escape local metastable states and reach states with lower potential energy. But when the temperature is too high, the transitions are random, and on average, there is no net energetic gain. Precisely this behavior is observed in panel (c) of Fig. 3. The average difference between a particle's energy before and after a transition, i.e., $\langle \Delta E \rangle$, grows with temperature until it saturates at $\langle \Delta E \rangle = 0$. So while the rare transitions at low temperatures occur toward (on average) lower energy states, very frequent transitions do not contribute anything at high temperatures. When average energetic gain, $\langle \Delta E \rangle$, is measured as a function of vibration frequency (for a fixed temperature), a contradiction with the previously described intuition is observed. Figure 3(d) shows that $|\langle \Delta E \rangle|$ always grow with vibration frequency. From this behavior, we can conclude that the effect of local noise due to substrate modifications is different on the single-particle level. Substrate modifications always provide favorable energetic pathways. These energetic pathways can lead to an improvement in cluster compactness, as is observed in Fig. 2(b).

We define the optimal vibration frequency $F(T)$ as the vibration frequency for which at temperature T the cluster compactness measure attains a minimum. Figure 4 presents $F(T)$ as a function of k_BT/J.

Figure 4 displays that it is always beneficial to introduce local noise, and the optimal amount of this noise grows with temperature. This growth supports the assumption that we raised above regarding different energetic pathways created due to the presence of local noise. The impact of the two noises differs quantitatively and qualitatively; they are not interchangeable.

IV. DISCUSSION

This study explored the self-assembly process on top of a 2D amorphous material that lacks periodicity. This

lack of periodicity can soften some constraints that limit the self-assembly of crystals by imposing a variation of particle-particle interactions. Previous studies have shown that uniform [47] or local [45] alternation of particle-particle interaction accelerates the self-assembly process. In this line of studies, modification comes from a built-in feature that characterizes each component of the system such as the shape of the component [47] or the internal state of the component [45]. In our case, modification of particle-particle interaction appears due to substrate variation, i.e., liquidity. Substrate variations modify the local structure of the substrate and, as a consequence, alter the average positions of the particles on top of the substrate, which in turn change the particle-particle interaction. Since these modifications are random, we compare the impact of substrate variations to the effect of temperature, i.e., noise in the system. Similarly to thermal fluctuations, substrate modifications stimulate the transition of particles from one location to another. But unlike thermal fluctuations, the average energetic gain from such transitions does not wear out when the vibration frequency of the substrate is large. Despite this net energetic gain per particle, the effect on cluster compactness is quite similar for both noises. There is a specific temperature/vibration frequency for which U is minimal, and more noise is destructive. While large thermal fluctuations cause random transitions that destabilize the cluster, large substrate variations can rip the cluster apart by disconnecting local neighbors. These modifications effectively increase particle energy, making the following transitions energetically favorable for the particle, but might not be perfect for the cluster formation. We can say that while temperature fluctuations facilitate transitions on top of a fixed energy landscape, substrate vibrations cause time-dependent deformations to this landscape. These deformations provide additional energetic pathways toward better self-assembly, up to a specific frequency of deformations. When these deformations of the energetic landscape are present, the system is out of equilibrium. Equilibrium relaxation on the energetic landscape formed during the nonequilibrium period leads to better self-assembly (i.e., more compact cluster). We find that it is always preferable to impose substrate variations, i.e., time-dependent deformations to the energy landscape (this occurs even when Voronoi dynamics is modified; see the Supplemental Material [41]). When the two noises are applied in a cohort, there is a preferable frequency of variations for any temperature. Moreover, this frequency monotonically grows with temperature, suggesting that the higher the thermal fluctuations are, the larger the amount of substrate variations that is needed.

Thus, behavior on the single-particle level, faster relaxation towards more compact cluster, and consistent improvement of the cluster due to additional frequency of vibrations (that grows with the temperature) advocate for a qualitative difference between the observed behavior and annealing due to temperature. Additional heating of the sample is known to produce faster freezing, e.g., the Mpemba effect, for which one of the explanations suggests faster search on top of a constant energy landscape occurs due to better initial spread achieved due to preheating [48]. In our case, it is not only that the self-assembly relaxes faster after substrate variations, but it also reaches more compact clusters. The search for the compact cluster occurs not only on a given energy landscape; imposed variations generate a search between different energy landscapes as well. The lack of periodicity of the 2D amorphous substrate allows us to perform this search among different energy landscapes in the first place. When the substrate is not constrained by crystalline order, local modifications are possible. These modifications change the energy landscape and effectively create two processes: one is on top of the energy landscape and the other is the transitions of the landscape itself. The observed amplification of self-assembly can appear due to effective cooperation, as in the case of stochastic resonance [49]. Our results will be beneficial not only for designers of self-assembly on top of 2D amorphous materials but also for any search process driven by fluctuations on a constant energy landscape, such as evolution [50] and deep learning [51].

ACKNOWLEDGMENT

D.S. thanks E. Shimshoni, D. A. Kessler and E. Lazar for fruitful discussions. This work was supported by Israel Science Foundation Grant No. 2796/20.

[1] Z. Yang, J. Hao, and S. P. Lau, Synthesis, properties, and applications of 2D amorphous inorganic materials, J. Appl. Phys. **127**, 220901 (2020).

[2] H. Zhao, Q. Guo, F. Xia, and H. Wang, Two-dimensional materials for nanophotonics application, Nanophotonics **4**, 128 (2015).

[3] G. Fiori, F. Bonaccorso, G. Iannaccone, T. Palacios, D. Neumaier, A. Seabaugh, S. K. Banerjee, and L. Colombo, Electronics based on two-dimensional materials, Nat. Nanotechnol. **9**, 768 (2014).

[4] A. K. Geim and I. V. Grigorieva, Van der Waals heterostructures, Nature (London) **499**, 419 (2013).

[5] K. S. Novoselov, D. Jiang, F. Schedin, T. J. Booth, V. V. Khotkevich, S. V. Morozov, and A. K. Geim, Two-dimensional atomic crystals, Proc. Natl. Acad. Sci. USA **102**, 10451 (2005).

[6] Z. Ling, C. E. Ren, M. Q. Zhao, J. Yang, J. M. Giammarco, J. Qiu, M. W. Barsoum, and Y. Gogotsi, Flexible and conductive MXene films and nanocomposites with high capacitance, Proc. Natl. Acad. Sci. USA **111**, 16676 (2014).

[7] G. Yang, L. Li, W. B. Lee, and M. C. Ng, Structure of graphene and its disorders: A review, Sci. Technol. Adv. Mater. **19**, 613 (2018).

[8] R. Kappera, D. Voiry, S. E. Yalcin, B. Branch, G. Gupta, A. D. Mohite, and M. Chhowalla, Phase-engineered low-resistance contacts for ultrathin MoS_2 transistors, Nat. Mater. **13**, 1128 (2014).

[9] Z. Cai, B. Liu, X. Zou, and H. M. Cheng, Chemical vapor deposition growth and applications of two-dimensional materials and their heterostructures, Chem. Rev. **118**, 6091 (2018).

[10] X. Li *et al.*, Large-area synthesis of high-quality and uniform graphene films on copper foils, Science **324**, 1312 (2009).

[11] J. H. Park and T. S. Sudarshan, *Chemical Vapor Deposition* (ASM International, Materials Park, OH, 2001).

[12] P. Zhang, X. Zheng, S. Wu, J. Liu, and D. He, Kinetic Monte Carlo simulation of Cu thin film growth, Vacuum **72**, 405 (2004).
[13] L. Meng, Q. Sun, J. Wang, and F. Ding, Molecular dynamics simulation of chemical vapor deposition graphene growth on Ni (111) surface, J. Phys. Chem. B **116**, 6097 (2012).
[14] Z. Chen, Y. Zhu, S. Chen, Z. Qiu, and S. Jiang, The kinetic process of non-smooth substrate thin film growth via parallel Monte Carlo method, Appl. Surf. Sci. **257**, 6102 (2011).
[15] M. Meixner, E. Schöll, V. A. Shchukin, and D. Bimberg, Self-Assembled Quantum Dots: Crossover from Kinetically Controlled to Thermodynamically Limited Growth, Phys. Rev. Lett. **87**, 236101 (2001).
[16] L. Pyziak, I. Stefaniuk, I. Virt, and M. Kuzma, Monte Carlo simulation of CdTe layers growth on CdTe(001) and Si(001) substrates, Appl. Surf. Sci. **226**, 114 (2004).
[17] L. Nurminen, A. Kuronen, and K. Kaski, Kinetic Monte Carlo simulation of nucleation on patterned substrates, Phys. Rev. B **63**, 035407 (2000).
[18] D. Schwarcz and S. Burov, The effect of disordered substrate on crystallization in 2D, J. Phys.: Condens. Matter **31**, 445401 (2019).
[19] D. Geng, B. Wu, Y. Guo, L. Huang, Y. Xue, J. Chen, G. Yu, L. Jiang, W. Hu, and Y. Liu, Uniform hexagonal graphene flakes and films grown on liquid copper surface, Proc. Natl. Acad. Sci. USA **109**, 7992 (2012).
[20] M. Zeng, L. Tan, J. Wang, L. Chen, M. H. Rümmeli, and L. Fu, Liquid metal: An innovative solution to uniform graphene films, Chem. Mater. **26**, 3637 (2014).
[21] T. Boeck, F. Ringleb, and R. Bansen, Growth of crystalline semiconductor structures on amorphous substrates for photovoltaic applications, Cryst. Res. Technol. **52**, 1600239 (2017).
[22] K. Zhang, X. B. Pitner, R. Yang, W. D. Nix, J. D. Plummer, and J. A. Fan, Single-crystal metal growth on amorphous insulating substrates, Proc. Natl. Acad. Sci. USA. **115**, 685 (2018).
[23] D. Chen, Y. Zheng, L. Liu, G. Zhang, M. Chen, Y. Jiao, and H. Zhuang, Stone–Wales defects preserve hyperuniformity in amorphous two-dimensional networks, Proc. Natl. Acad. Sci. USA **118**, e2016862118 (2021).
[24] A. J. Stone and D. J. Wales, Theoretical studies of icosahedral C60 and some related species, Chem. Phys. Lett. **128**, 501 (1986).
[25] F. Iacopi *et al.*, Short-ranged structural rearrangement and enhancement of mechanical properties of organosilicate glasses induced by ultraviolet radiation, J. Appl. Phys. **99**, 053511 (2006).
[26] R. Klajn, K. J. M. Bishop, and B. A. Grzybowski, Light-controlled self-assembly of reversible and irreversible nanoparticle suprastructures, Proc. Natl. Acad. Sci. USA **104**, 10305 (2007).
[27] J. Kotakoski, A. V. Krasheninnikov, U. Kaiser, and J. C. Meyer, From Point Defects in Graphene to Two-Dimensional Amorphous Carbon, Phys. Rev. Lett. **106**, 105505 (2011).
[28] M. Grzelczak, J. Vermant, E. M. Furst, and L. M. Liz-Marza, Directed self-assembly of nanoparticles, ACS Nano **4**, 3591 (2010).
[29] M. O. Blunt, J. Adisoejoso, K. Tahara, K. Katayama, M. Van der Auweraer, Y. Tobe, and S. De Feyter, Temperature-induced structural phase transitions in a two-dimensional self-assembled network, J. Am. Chem. Soc. **135**, 12068 (2013).
[30] K. Momeni *et al.*, Multiscale computational understanding and growth of 2D materials: A review, npj Comput. Mater. **6**, 22 (2020).
[31] F. Elsholz, E. Schöll, and A. Rosenfeld, Control of surface roughness in amorphous thin-film growth, Appl. Phys. Lett. **84**, 4167 (2004).
[32] W. K. Burton, N. Cabrera, and F. C. Frank, The growth of crystals and the equilibrium structure of their surfaces, Philos. Trans. R. Soc. London A **243**, 299 (1951).
[33] G. H. Gilmer and P. Bennema, Simulation of crystal growth with surface diffusion, J. Appl. Phys. **43**, 1347 (1972).
[34] M. Kardar, G. Parisi, and Y. C. Zhang, Dynamic Scaling of Growing Interfaces, Phys. Rev. Lett. **56**, 889 (1986).
[35] M. J. Patitz, An introduction to tile-based self-assembly and a survey of recent results, Nat. Comput. **13**, 195 (2014).
[36] Y. Brun, Arithmetic computation in the tile assembly model: Addition and multiplication, Theor. Comput. Sci. **378**, 17 (2007).
[37] A. Chatterjee and D. G. Vlachos, An overview of spatial microscopic and accelerated kinetic Monte Carlo methods, J. Comput.-Aided. Mater. **14**, 253 (2007).
[38] M. Biehl, Lattice gas models and kinetic Monte Carlo simulations of epitaxial growth, Int. Ser. Numer. Math. **149**, 3 (2005).
[39] G. O. Jordi and J. M. Sancho, in *Noise in Spatially Extended Systems* (Springer, New York, 1999), pp. 1–10.
[40] D. Chandler, J. D. Weeks, and H. C. Andersen, Van der Waals picture of liquids, solids, and phase transformations, Science **220**, 787 (1983).
[41] See Supplemental Material at http://link.aps.org/supplemental/10.1103/PhysRevE.105.L022601 for Gaussian noise simulation details and Voronoi tessellation picture explanation and updates.
[42] C. Moukarzel and H. J. Herrmann, A vectorizable random lattice, J. Stat. Phys. **68**, 911 (1992).
[43] C. J. O'Keeffe and G. Orkoulas, Parallel canonical Monte Carlo simulations through sequential updating of particles, J. Chem. Phys. **130**, 134109 (2009).
[44] G. Kabbe, C. Wehmeyer, and D. Sebastiani, A coupled molecular dynamics/kinetic Monte Carlo approach for protonation dynamics in extended systems, J. Chem. Theory Comput. **10**, 4221 (2014).
[45] G. Bisker and J. L. England, Nonequilibrium associative retrieval of multiple stored self-assembly targets, Proc. Natl. Acad. Sci. USA **115**, E10531 (2018).
[46] M. C. Rechtsman, F. H. Stillinger, and S. Torquato, Optimized Interactions for Targeted Self-Assembly: Application to a Honeycomb Lattice, Phys. Rev. Lett. **95**, 228301 (2005).
[47] T. D. Nguyen, E. Jankowski, and S. C. Glotzer, Self-assembly and reconfigurability of shape-shifting particles, ACS Nano **5**, 8892 (2011).
[48] Z. Lu and O. Raz, Nonequilibrium thermodynamics of the Markovian Mpemba effect and its inverse, Proc. Natl. Acad. Sci. USA **114**, 5083 (2017).
[49] L. Gammaitoni, P. Hänggi, P. Jung, and F. Marchesoni, Stochastic resonance, Rev. Mod. Phys. **70**, 223 (1998).
[50] Y. Guo, M. Vucelja, and A. Amir, Stochastic tunneling across fitness valleys can give rise to a logarithmic long-term fitness trajectory, Sci. Adv. **5**, 3842 (2019).
[51] A. J. Ballard, R. Das, S. Martiniani, D. Mehta, L. Sagun, J. D. Stevenson, and D. J. Wales, Energy landscapes for machine learning, Phys. Chem. Chem. Phys. **19**, 12585 (2017).